

# Intelligent Mode-Locked Single-Cavity Dual-Comb Laser Utilizing Time-Stretch Dispersive Fourier Transform Spectroscopy with Supplemental File

Pan Guo, Yuan Gao, Yongjie Pu, Zhigang Zhao, Zhenhua Cong and Sha Wang\*

**Abstract**—As dual combs play a significant role in numerous high-precision measurements, their efficient generation has been widely researched. Although the single-cavity dual-comb generation can avoid the complex active stabilization methods, achieving and maintaining stable dual-comb mode locking within a single cavity remains a critical challenge. To break through this constraint, a two-part evaluation criterion containing a fitness function and a CNN-Transformer network is employed to achieve mode locking and classify the dual-comb mode-locked state. Simulated time-stretch dispersive Fourier transform (DFT) spectra are used as datasets, which simplifies the optimization process and does not rely on specific experimental data. A developed evolutionary algorithm (EA) for paddle-based motorized polarization controllers (MPCs) is proposed, enabling the intelligent attainment of dual-comb mode-locked states. A real-time library stores fitness and MPC angles, facilitating mode-locked state achievement within 2 seconds. Finally, long term running of dual-comb mode locking is ensured by a random collision algorithm utilizing an evaluation criterion of weak soliton peaks.

**Index Terms**—dual-comb mode locking, Lyot filter, time-stretch DFT, evolutionary algorithm, neural network

## I. INTRODUCTION

DUAL-COMB technologies involve utilizing two coherent optical pulse trains with a small frequency difference in their repetition rates, which can offer capabilities for fast measurements, high resolution, and high sensitivity in the fields of precise ranging [1-2] and molecular spectroscopy [3-4]. Normally, the realization of dual combs generally requires two separate and mutually coherent mode-locked lasers, which makes the source expensive, complicated, and bulky. To broaden the applicability of dual-comb technology, in 2008, K. Kieu proposed the first all-fiber bidirectional single-cavity, Erbium-doped ring-shaped laser, offering a more compact and cost-efficient solution for

This work was supported by the National Natural Science Foundation of China (Grant Nos. 62475175), Opening Foundation of Key Laboratory of Laser & Infrared System (Shandong University), Ministry of Education.

Pan Guo, Yuan Gao, Yongjie Pu, and Sha Wang are with the College of Electronics and Information Engineering, Sichuan University, 610064, Chengdu, China.

Zhigang Zhao, Zhenhua Cong are with the School of Information Science and Engineering, and Shandong Provincial Key Laboratory of Laser Technology and Application, Shandong University, 266237, Qingdao, China.

\* Corresponding author: Sha Wang (email: shawang@scu.edu.cn)

generating dual combs [5]. Compared to combining two independent optical combs, employing a single-cavity dual-comb laser eliminates the need for additional stabilization approaches to lock the phases of the two pulse trains. Moreover, since these two mode-locked pulse trains share a common laser cavity, a high mutual coherence is achieved due to common-mode noise cancellation [6].

The primary methods for generating single-cavity dual combs fundamentally rely on the concept of "multiplexing", wherein the cavity is constructed to permit the simultaneous oscillation of pulses with distinct characteristics along a single propagation dimension [7], such as wavelength-multiplexing [8-9], polarization-multiplexing [10-11], direction-multiplexing [12-13], and pulse shape-multiplexing [14]. And the wavelength-multiplexing is a straightforward approach to augmenting the optical channel capacity in fiber lasers. However, the generation of single-cavity dual combs with these methods always relies on manual adjustments including precise control of intracavity polarization and gain-to-loss ratio [15]. The intricate interplay of intracavity dispersion, nonlinear dynamics, and environmental perturbations collectively induces instability in the dual-comb formation. Thus, establishing and maintaining the dual-comb mode locking within a single cavity remains a challenge, which restricts the practical utility of dual combs.

In response to these challenges, intelligent mode-locked techniques based on artificial intelligence and electric polarization controllers have been developed. Recently, genetic algorithms, deep reinforcement learning, and neural networks have been extensively applied to the intelligent control of ultrafast fiber lasers, and they have enhanced their reliability and efficiency in various applications [16-18]. In the process of intelligent mode locking, real-time acquisition of the current laser output spectrum is beneficial for accurately assessing the state of the laser system. Reinforcement learning emphasizes interaction with the environment, and by receiving rewards from the reward function, the optimal policy can be learned [19-20]. In 2024, soft actor-critic (SAC) reinforcement learning was utilized by A. Kokhanovskiy et al. for generating a harmonic mode-locked regime. The training procedure lasted 45 hours and the SAC algorithm typically took six steps to adjust the voltage in about a minute [21]. This approach requires a long time in training, thus may not be suitable for certain applications [22]. Additionally, the complexity of the nonlinear dynamics in dual-comb mode locking causes difficulties in establishing evaluation criteria. Consequently,

most of the current research on intelligent mode locking focuses on single-wavelength systems, with relatively fewer studies on dual-wavelength systems. To the best of our knowledge, there are only two such studies currently. In 2023, G. Pu et al. demonstrated the first intelligent single-cavity dual-comb fiber laser by combining the real-time intelligent control and the memory-aided intelligent searching (MAIS) algorithm. Employing a field-programmable gate array (FPGA), and two digital-to-analog converters enabled MAIS can locate a desired solution in a mean time of only 2.48 seconds [23]. An oscilloscope and an optical spectrum analyzer (OSA) were used simultaneously to record temporal pulse trains and spectral information. Q. Yan et al. also reported an automatic mode locking in a dual-wavelength soliton fiber laser. By using a two-stage genetic algorithm, the laser kept a stable dual-wavelength mode locking for hours [24].

In this work, we report an intelligent single-cavity dual-comb mode-locked fiber laser based on time-stretch dispersive Fourier transform (DFT). To avoid the utilization of the bulky OSA with slow speed, an oscilloscope is used to receive DFT spectra in real time, which combines time-domain and spectral information. To elevate the performance of the laser output, a two-part evaluation criterion containing a fitness function and a CNN-Transformer network is utilized. It ensures that both global and local characteristics of the time-stretch spectrum are comprehensively considered, which leads to a more accurate assessment of various mode-locked states. The utilized datasets exclusively consist of synthetically generated time-stretch DFT spectra, that can leave out the early collection of empirical data and improve the universality of the model. Based on the evaluation criterion, a developed EA is proposed to achieve intelligent mode locking of the dual-comb state. This EA is designed to electronically drive the paddle-based motorized polarization controllers (MPCs) and enable the optimal six-parameter search with a fitness function. The employed fitness function is capable of locating dual-comb mode locking. High-order harmonic mode locking can be accurately distinguished according to their spectral information. During the process of searching different mode-locked states automatically, a mode-locking library supporting real-time updates is built, which includes different mode-locked states, fitness functions, and angles of each paddle in the current state. The establishment of the mode-locked library allows the direct location of various mode-locking states without repeating the optimization algorithm. Multiple experiments have shown that the mode-locked library can be established within 15 minutes. Subsequently, the saved angles in the library can be directly used to achieve the corresponding dual comb mode-locked states, with an average time of less than 2 seconds, which is the fastest record according to our best knowledge.

## II. EXPERIMENTAL SETUP OF THE INTELLIGENT DUAL-COMB FIBER LASER

The configuration of the intelligent dual-comb fiber laser is shown in Figure 1. The fiber laser is based on an all-fiber ring-

cavity mode-locked with a nonlinear polarization rotation (NPR). A 2.5-m polarization-maintaining erbium-doped fiber (PM-EDF) with a calculated second-order dispersion of  $28 \text{ ps}^2/\text{km}$  constitutes the gain medium, pumped by a 980-nm laser diode through a 980/1550 wavelength division multiplexer (WDM). A polarization-dependent isolator (PD-ISO) ensures the unidirectional transmission of light in the fiber. The maximum rotation speed can reach  $400^\circ/\text{sec}$  with open loop operation. Moreover, in order to obtain dual-comb mode locking with asynchronous pulse trains, a specific intracavity optical filtering effect should be established. In this laser cavity, a separate PBS-PMF-PC structure is adopted. The polarization-dependent loss of the PBS and PC combined with the birefringence from 30-cm polarization-maintaining fibers can produce the Lyot filtering effect. And the formation of dual-comb pulse trains is significantly influenced by the dual-wavelength net gain spectrum, which depends on the balance of gain, loss, and the filtering effect. The total length of the laser cavity is  $\sim 17 \text{ m}$ , corresponding to the fundamental repetition rate of  $\sim 12 \text{ MHz}$ . The net cavity dispersion is  $\sim 0.308 \text{ ps}^2$  at 1550 nm which means the mode-locked laser operates in the anomalous regime. Approximately 90% of the laser energy stays within the ring cavity by using an output coupler (OC), while the rest is utilized for characterizing laser mode-locked states and feedback control.

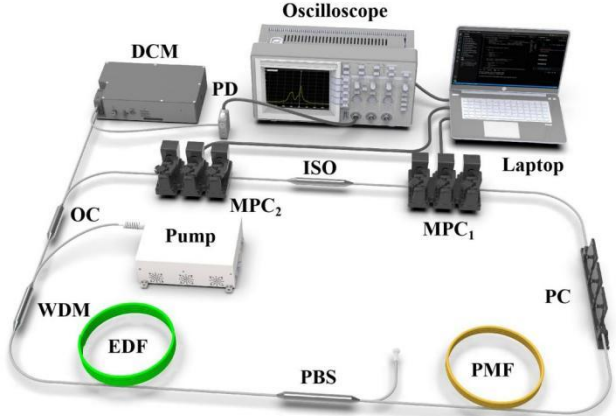


**Fig. 1.** The experimental setup of the intelligent single-cavity dual-comb mode-locked laser.

The output laser is propagated through a time-stretch DFT setup containing a dispersion compensation module (DCM) which provides a total accumulated dispersion of  $DL = -654 \text{ ps/nm}$ . After that, the laser pulse will get stretched considerably, in order that the spectral information is mapped into the time-domain trains. A balance photodetector is used to detect the time-stretch DFT output signal, temporal pulse trains containing spectral information can be captured directly on the oscilloscope, with a resolution of  $\Delta\lambda = 1 / (DL \times BW) = 0.3 \text{ nm}$ , where  $BW$  is the bandwidth of the balance photodetector. A laptop that runs EA and is connected to the oscilloscope can receive pulse signals in real time. And then it sends new control commands generated by the EA to electrically control six paddles of the two MPCs directly to achieve polarization control.

### III. PROCESS OF THE INTELLIGENT SEARCHING

#### A. Two-part evaluation criterion

Establishing an excellent evaluation criterion is the key premise of intelligent search. The evaluation criterion of the individual's competitiveness has two parts: fitness function and neural network classification. Firstly, regarding the fitness function, it is observed that dual-comb mode locking may be achieved directly in the rare chance. Therefore, a dual-comb fitness function is also evaluated together with the single-wavelength fitness. When the laser output is closer to the target state, the fitness corresponds to a higher value. We are looking for the parameters that generate solutions with the maximum total pulse energy, the number of stable pulses in the same time window, and noise intensity. The dual-region count scheme is adopted to judge the pulse trains preliminary [25]. Moreover, two intensity thresholds  $T_1$  and  $T_2$  are set,

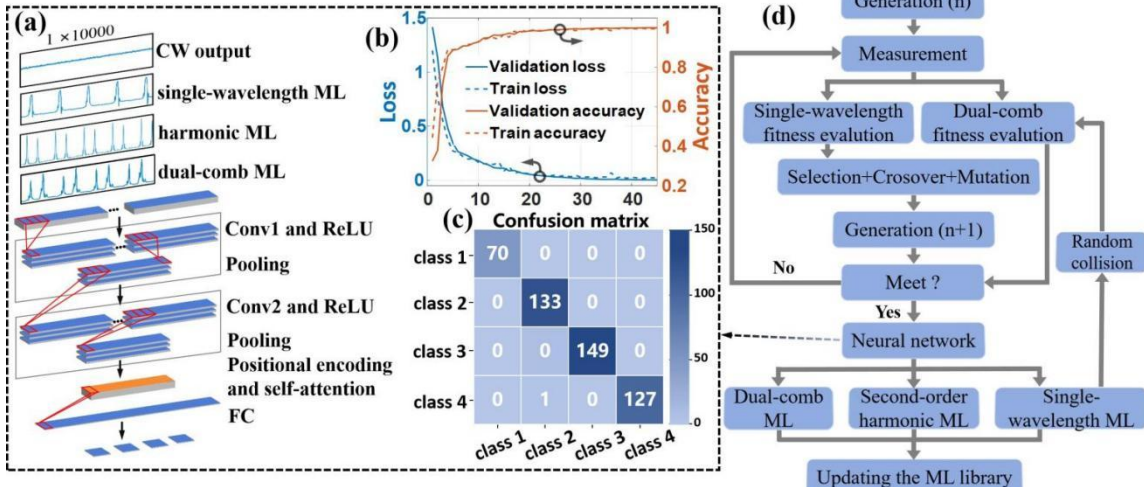


**Fig. 2.** (a) The classification network structure of the CNN-Transformer network. (b) The curves of the loss and accuracy over epochs in the training process. (c) Confusion matrix for the CNN-Transformer network of 4 classifications. Class 1 through 4 correspond to continuous wave (CW), single-wavelength, harmonic, and dual-comb mode locking, respectively. (d) The principle of the developed EA for achieving different states of mode locking containing single-wavelength, second-order harmonic, and dual-comb mode locking.

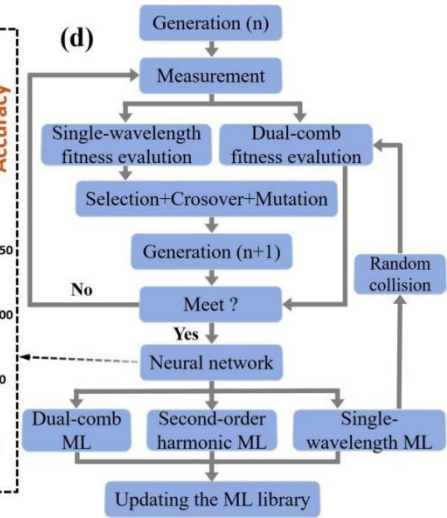
where  $T_1 > T_2$ .  $T_1$  is built for the desired pulse count.  $T_2$  is a limitation that noise should not surpass. Specifically, the DFT spectrum on the oscilloscope greater than  $T_1$  is considered as effective pulses, and those less than  $T_2$  are considered as noises. The fitness function can be constructed as follows:

$$Fitness = I_{pulse} - \alpha |C_{real} - C_{ideal}| - \beta I_{noise} \quad (1)$$

Where the first term of the fitness is the sum intensity of the pulse  $I_{pulse}$  within a fixed time window; The second term represents the deviation punishment for the pulse count with a scale factor  $\alpha$ , where  $C_{real}$  and  $C_{ideal}$  denote the real pulse count and the ideal pulse count of target mode-locked state, respectively; The third term stands for the punishment of noise  $I_{noise}$  and its weight  $\beta$ , which can show the stability of the current mode-locked state to a certain extent. The record length and acquisition time of the oscilloscope are 10K Sa and 400 ns, respectively.

However, in the dual-comb mode-locked state, the two temporal pulse trains periodically overlap because of the temporal asynchrony. As a result, certain dual-comb signals on the oscilloscope will appear to be very similar to those of single-wavelength mode-locked states. Such minor discrepancies will reduce the evaluating accuracy of the fitness function. Moreover, harmonic mode locking is also observed during the intelligent adjustment. In particular, the pulse trains of the second-order harmonic and dual-comb mode locking are very similar, this makes it difficult to efficiently distinguish with the fitness function.

Therefore, the second evaluation of the individual's competitiveness, a CNN-Transformer network, is proposed to classify the one-dimensional time-stretch DFT spectra in time domain. The training datasets of the CNN-Transformer network are completely provided by numerical simulations of the Ginzburg-Landau equation [26]:



$$\frac{\partial u}{\partial z} + i \frac{\beta_2}{2} \frac{\partial^2 u}{\partial T^2} = i\gamma|u|^2 u + \frac{g}{2}u + \frac{g}{2Q_g^2} \frac{\partial^2 u}{\partial T^2} \quad (2)$$

where  $u$  is the complex envelop of the pulse trains, the attenuation coefficient of fiber  $\alpha = 0.3$ . The continuous wave output can be generated by background noise with different intensities. The DFT spectra generated by computer simulation can replace the signal collected in the experiment very well, as presented in Supplemental File Section S1.

The network structure is shown in Figure 2(a). The accuracy and loss results of the train and validation are demonstrated in Figure 2(b). Because of the different spectral characteristics of harmonic mode-locked pulses and dual-comb mode-locked pulses, it can be clearly mapped to the oscilloscope after time stretch, see Supplementary Section S2 for details. The accuracy of the validation sets of the model reaches 99.79% within 50 epochs, while the accuracy of the training sets is 100%. From the confusion matrix depicted in

Figure 2(c), it can be observed that the periodic overlap resulting from temporal asynchrony occasionally presents a challenge to its correct classification.

### B. Principle of the developed EA

According to the proposed evaluation criterion, the intelligent searching of different mode-locked states is achieved via a developed EA, and the detailed algorithmic frame is shown in Figure 2(d). In our case, the optimization algorithm, neural network classification, and the mode-locked library building or updating are tightly fused, so that the searching speed and accuracy are enhanced. EA is a class of optimization techniques inspired by the principles of biological evolution, and it is characterized by their ability to handle a wide range of optimization problems, including those with large search spaces and complex fitness landscapes [27].

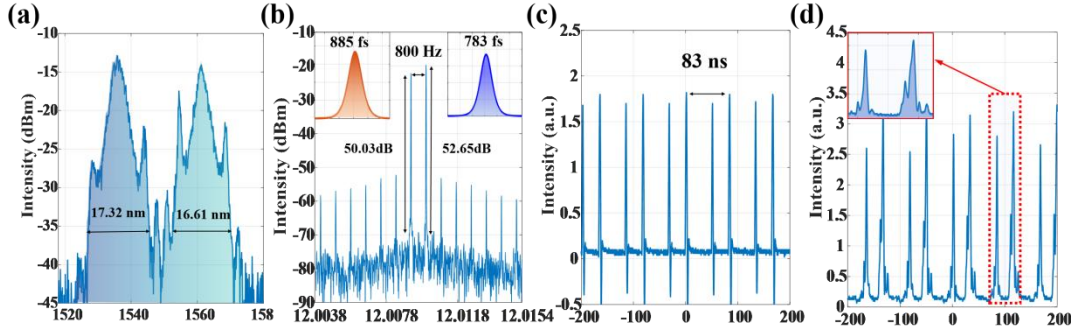


**Fig. 3.** Output characteristics of the intelligent dual-comb fiber laser. (a) Optical spectrum of the dual-comb mode-locked state. (b) RF spectrum with beat frequency, the left and right insets present the autocorrelation trace of solitons centered at 1536 nm and 1561 nm, respectively. (c) Time-domain pulse trains of the dual-comb mode-locked state. (d) Time-stretch DFT spectrum, inset: local view of a peak in a single period.

### C. Building mode-locked library

To prevent repetitive searching of mode locking in the same laser, we build a library containing the fitness function for different stable mode-locked states and the six angles of MPCs. The data in the library supports real-time updating of new mode-locked states and reading of all states. Depending on the initial angles of MPCs' paddles, after multiple experiments, it is verified that the library can be built up within 15 minutes. Reading the saved angles can directly achieve the corresponding mode-locked state, with an average time of less than 2 seconds.

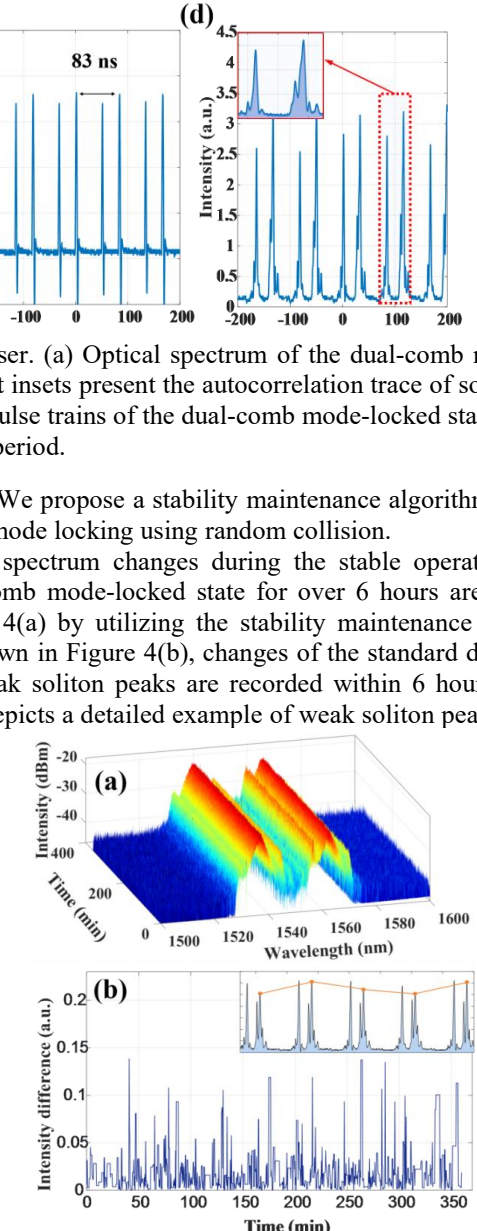
## IV. LASER PERFORMANCE

Figure 3 depicts the output characteristics of the intelligent dual-comb fiber laser. As shown in Figure 3(a), the spectral widths of separated mode-locked pulses with central wavelengths of 1536.83 nm and 1561.26 nm are 17.32 nm and 16.61 nm, respectively. Due to the significant differences in optical spectra, we have found that using the different single-wavelength time-stretch DFT spectra collected in the experiment can also achieve the classification of different single-wavelength mode-locked states, see Supplemental File Section S3 for details. The RF spectrum can be seen in Figure 3(b), two repetition-rate signals can be found around 12.0 MHz, and the corresponding repetition-rate difference is about

800 Hz. The employment of the Lyot filter allows for the realization of single soliton mode locking at a higher pump power [9], so the phenomenon of multiple solitons caused by pulse splitting is not observed. The temporal oscilloscope waveform of the dual-comb pulses is shown in Figure 3(c). Figure 3(d) displays the one-dimensional spectra after time-stretch DFT.

## V. STABILITY MAINTENANCE

Besides ensuring that intelligent algorithms can efficiently search for and classify various mode-locked states, maintaining the stability of these states over prolonged operation is equally crucial. The spectrum changes of the mode-locked states at the central wavelengths of 1536 nm and 1561 nm can be seen in Supplemental File Section S4 for details. They are easy to maintain the operation for over 6



**Fig. 4.** (a) The stability maintenance results of dual-comb mode locking. (b) Changes of the standard deviation of pulse

peak values in the process of stability maintenance, inset: details of the soliton peak selection.

## VI. CONCLUSION

In this work, we demonstrate an intelligent single-cavity dual-comb mode-locked fiber laser. A two-part evaluation criterion containing a fitness function and a CNN-Transformer network is proposed to elevate dual-comb mode-locked states. The input datasets corresponding to various mode-locked states are obtained by simulation, which circumvents the need for over-reliance on specific experimental datasets. Then a developed EA is utilized to optimize the fitness function and control paddle-based MPCs to find the desired mode-locked state. After that, a library supporting real-time updating and reading is built to store the fitness functions for different stable mode-locked states and the six angles of MPCs. The mode-locked library can be set up within a 15-minute duration. Reading the saved angles can directly achieve the corresponding mode-locked state, with an average time of less than 2 seconds. In addition, a new evaluation criterion combined with a random collision algorithm is used to achieve the stable maintenance of the dual-comb mode locking. For subsequent work, we plan to further study the intelligent control and stability of the frequency of the dual-comb laser, and apply it to practical applications such as absorption spectrum measurement and fiber sensing.

## REFERENCES

- [1] E. D. Caldwell, L. C. Sinclair, N. R. Newbury, and J. Deschenes, “The time-programmable frequency comb and its use in quantum-limited ranging,” *Nature*, vol. 610, no. 7933, pp. 667-673, Oct. 2022, doi: 10.1038/s41586-022-05225-8.
- [2] J. Fellinger, *et al.*, “Simple approach for extending the ambiguity-free range of dual-comb ranging,” *Optics Letters*, vol. 46, no. 15, pp. 3677-3680, Aug. 2021, doi: 10.1364/OL.427816.
- [3] B. Cho, T. H. Yoon, and M. Cho, “Dual-comb spectroscopy of molecular electronic transitions in condensed phases,” *Physical Review A*, vol. 97, no. 3, pp. 033831, Mar. 2018, doi: 10.1103/PhysRevA.97.033831.
- [4] G. Millot *et al.*, Frequency-agile dual-comb spectroscopy. *Nature Photonics*, vol. 10, no. 1, pp. 27-30, Dec. 2016, doi: 10.1038/nphoton.2015.250.
- [5] K. Kieu, and M. Mansuripur, “All-fiber bidirectional passively mode-locked ring laser,” *Optics Letters*, vol. 33, no. 1, pp. 64-66, Jan. 2008, doi: 10.1364/OL.33.000064.
- [6] Z. Wang, *et al.*, “Cavity-enhanced photoacoustic dual-comb spectroscopy,” *Light: Science & Applications*, vol. 13, no. 1, pp. 11, Jan. 2024, doi: 10.1038/s41377-023-01353-6.
- [7] X. Zhao, Z. Zheng, Y. Liu, G. Hu, and J. Liu, “Dual-wavelength, bidirectional single-wall carbon nanotube mode-locked fiber laser,” *IEEE Photonics Technology Letters*, vol. 26, no. 17, pp. 1722-1725, Jun. 2014, doi: 10.1109/LPT.2014.2332000.
- [8] Y. Pu, M. Fan, Q. Shen, P. Guo, Y. Gao, and S. Wang, “Mode-locking and wavelength-tuning of a NPR fiber laser based on optical speckle,” *Optics Letters*, vol. 49, no. 13, pp. 3686-3689, Jul. 2024, doi: 10.1364/OL.528656.
- [9] Y. Pu, *et al.*, “Yb-doped mode-locked fiber laser with a hybrid structure of NPR and a Lyot filter as the saturable absorber,” *Optics Letters*, vol. 49, no. 8, pp. 2149-2152, Apr. 2024, doi: 10.1364/OL.516495.
- [10] Z. Ding, G. Wang, and F. Xu, “Highly birefringent D-shaped micro-fiber device for high-repetition-rate-difference single-cavity dual-comb generation,” *Journal of Lightwave Technology*, vol. 42, no. 10, pp. 3877-3883, Feb. 2024, doi: 10.1109/JLT.2024.3368514.
- [11] M. Kowalczyk, Ł. Sterczewski, X. Zhang, V. Petrov, Z. Wang, and J. Sotor, “Dual-comb femtosecond solid-state laser with inherent polarization-multiplexing,” *Laser & Photonics Reviews*, vol. 15, no. 8, pp. 2000441, Jun. 2021, doi: 10.1002/lpor.202000441.
- [12] Y. Liu, *et al.*, “Self-starting and repetition-rate-difference tunable dual combs in a bidirectional mode-locked fiber laser,” *Optics & Laser Technology*, vol. 177, pp. 111178, Oct. 2024, doi: 10.1016/j.optlastec.2024.111178.
- [13] N. Prakash, S. W. Huang, and B. Li, “Relative timing jitter in a counterpropagating all-normal dispersion dual-comb fiber laser,” *Optica*, vol. 9, no. 7, pp. 717-723, Jul. 2022, doi: 10.1364/OPTICA.458339.
- [14] Y. Liu, X. Zhao, G. Hu, C. Li, B. Zhao, and Z. Zheng, “Unidirectional, dual-comb lasing under multiple pulse formation mechanisms in a passively mode-locked fiber ring laser,” *Optics Express*, vol. 24, no. 19, pp. 21392-21398, Sep. 2016, doi: 10.1364/OE.24.021392.
- [15] U. Andral, R. S. Fodil, F. Amrani, and F. Billard, “Fiber laser mode locked through an evolutionary algorithm,” *Optica*, vol. 2, no. 4, pp. 275-278, Mar. 2015, doi: 10.1364/OPTICA.2.000275.
- [16] P. Guo, M. Fan, H. Li, K. Liu, Y. Pu, and S. Wang, “Intelligent laser emitting and mode locking of solid-state lasers using human-like algorithms,” *Laser & Photonics Reviews*, vol. 18, no. 8, pp. 2301209, Apr. 2024, doi: 10.1002/lpor.202301209.
- [17] J. Girardot, F. Billard, A. Collet, É. Hertz, and P. Grelu, “Autosetting mode-locked laser using an evolutionary algorithm and time-stretch spectral characterization,” *IEEE Journal of Selected Topics in Quantum Electronics*, vol. 26, no. 5, pp. 1-8, Apr. 2020, doi: 10.1109/JSTQE.2020.2985297.
- [18] J. Li, *et al.*, “The soft actor-critic algorithm for automatic mode-locked fiber lasers,” *Optical Fiber Technology*, vol. 81, pp. 103579, Dec. 2023, doi: 10.1016/j.yofte.2023.103579.
- [19] Q. Yan, *et al.*, “Low-latency deep-reinforcement learning algorithm for ultrafast fiber lasers,” *Photonics Research*, vol. 9, no. 8, pp. 1493-1501, Jun. 2021, doi: 10.1364/PRJ.428117.
- [20] C. Sun, E. Kaiser, S. L. Brunton and J. N. Kutz, “Deep reinforcement learning for optical systems: A case study of mode-locked lasers,” *Machine Learning: Science and Technology*, vol. 1, no. 4, pp. 045013, Oct. 2020, doi: 10.1088/2632-2153/abb6d6.
- [21] A. Kokhanovskiy, *et al.*, “Multistability manipulation by reinforcement learning algorithm inside mode-locked fiber laser,” *Nanophotonics*, vol. 13, no. 16, pp. 2891-2901, Apr. 2024, doi: 10.1515/nanoph-2023-0792.
- [22] F. Edoardo, H. A. Loughlin, and C. Stoughton, “Controlling optical-cavity locking using reinforcement learning,” *Machine Learning: Science and Technology*, vol. 5, no. 3, pp. 035027, Jul. 2024, doi: 10.1088/2632-2153/ad638f.
- [23] G. Pu, R. Liu, C. Luo, Y. Song, H. Mu, and W. Hu, “Intelligent single-cavity dual-comb source with fast locking,” *Journal of Lightwave Technology*, vol. 41, no. 2, pp. 593-598, Nov. 2022, doi: 10.1109/JLT.2022.3220258.
- [24] Q. Yan, *et al.*, “Machine learning based automatic mode-locking of a dual-wavelength soliton fiber laser,” *Photonics*, vol. 11, no. 1, pp. 47, Dec. 2024, doi: 10.3390/photonics11010047.
- [25] G. Pu, L. Yi, L. Zhang, and W. Hu, “Intelligent programmable mode-locked fiber laser with a human-like algorithm,” *Optica*, vol. 6, no. 3, pp. 362-369, Mar. 2019, doi: 10.1364/OPTICA.6.000362.
- [26] Y. Lyu, J. Li, Y. Hu, Y. Wang, C. Wei, Y. Liu, “Theoretical comparison of NPR and hybrid mode-locked soliton thulium-doped fiber lasers,” *IEEE Photonics Journal*, vol. 9, no. 1, pp. 1-11, Jan. 2017, doi: 10.1109/JPHOT.2017.2653860.
- [27] T. Bäck, and H. P. Schwefel, “An overview of evolutionary algorithms for parameter optimization,” *Evolutionary computation*, vol. 1, no. 1, pp. 1-23, Mar. 1993, doi: 10.1162/evco.1993.1.1.1.

## Supplementary File

### S1. The time-stretch DFT spectra of dual comb generated by the computer

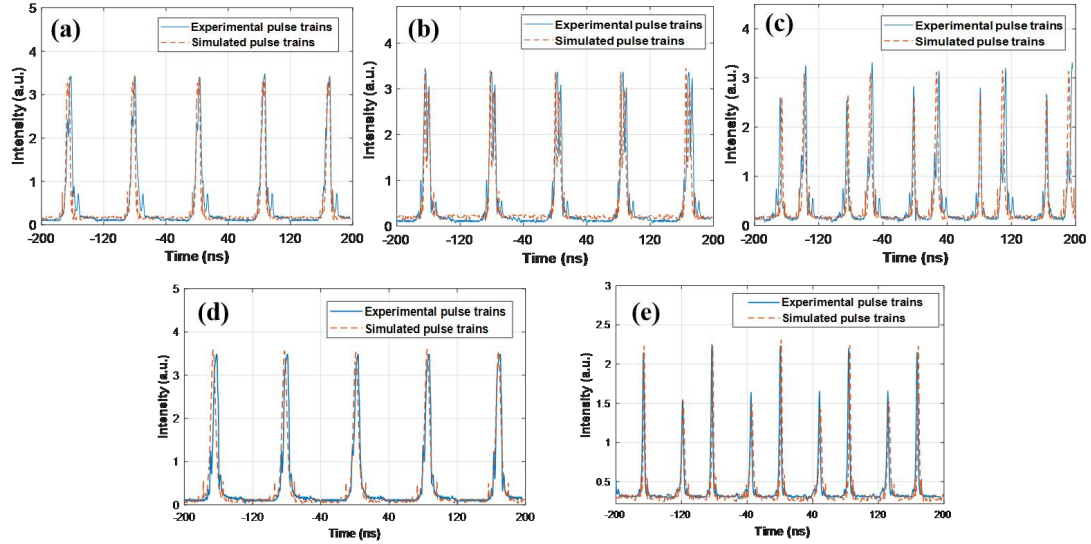


**Fig. S1.** Comparison of time-stretch DFT signals generated by computer simulation and experimental measurement. (a) Complete overlap, (b) partial overlap, (c) complete separation, (d) single-wavelength mode locking and (e) harmonic mode locking.

The time-stretch DFT spectra generated by the computer are compared with those collected in the experiment. Figure S1 (a), (b), and (c) select the cases where the time-stretch DFT spectra completely overlap, partially overlap, and completely separate, respectively. Figure S1 (d) and (e) select the time-stretch DFT spectra of single-wavelength mode locking and harmonic mode locking, respectively. It can be seen that the time-stretch DFT spectra generated by computer simulation can replace the signal collected by the experiment very well.

### S2. Time-stretch DFT spectrum of the harmonic mode-locked state

The measured second-order harmonic time-stretch DFT spectrum is shown in Figure S2(a), and it can be seen that they are very similar to the DFT spectra of dual-comb mode locking. Thus during the process of using the evolutionary algorithm with a fitness function of Equation (1), it is difficult to distinguish between dual-comb mode locking and second-order harmonic mode locking using only pulse count. Although harmonic mode locking has periodic pulse repetition in the time domain, unlike dual-comb mode locking, multiple pulses within the same period all have the same spectral information. After passing through the DCM, adjacent second-order harmonic mode locking time-stretch DFT pulses have similar profiles, as shown in Figure S2(b). In dual-comb mode locking, due to the different spectral information of two solitons within the same period, significant differences can be exhibited after time stretching, as shown in Figure S2(c).

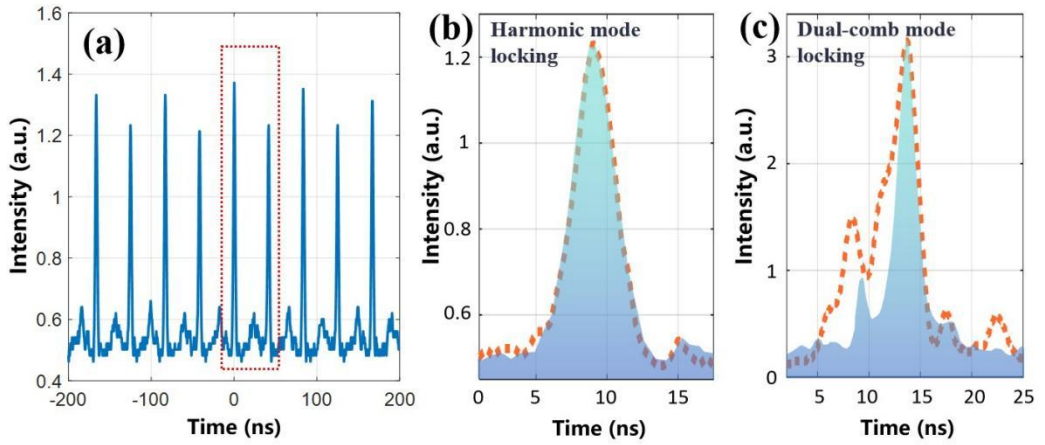


**Fig. S2.** (a) Time-stretch DFT spectrum of the harmonic mode-locked state. After normalization and shift processing, the overlapping curves of adjacent pulses of (b) harmonic mode locking and (c) dual-comb mode locking.

### S3. Classification of 1536-nm and 1561-nm single-wavelength mode-locked states

After the time stretch of the dispersion compensation module, these spectral characteristics will map to the DFT time-domain pulse trains. Benefiting from these characteristics, we also achieve the automatic tuning of single-wavelength mode locking with different central wavelengths. In the experiment, 800 DFT pulse trains with central wavelengths at 1536 nm and 1561 nm are collected, respectively. Combined with the previously simulated CW output, second-order harmonic and the dual-comb DFT pulse trains together as the input datasets, a 5-class neural network is trained without any changes to the network structure or hyperparameters. Figure S3(a) depicts that the accuracy of the validation sets of the model reaches 99.67% within 100 epochs, while the accuracy of the training sets is 100%. As shown in Figure S3(b), in addition to the periodic overlap of dual-comb pulse trains, the time-stretch signals of the single-wavelength mode locking centered at 1536 nm and 1561 nm are similar, which results in occasional errors in classification.

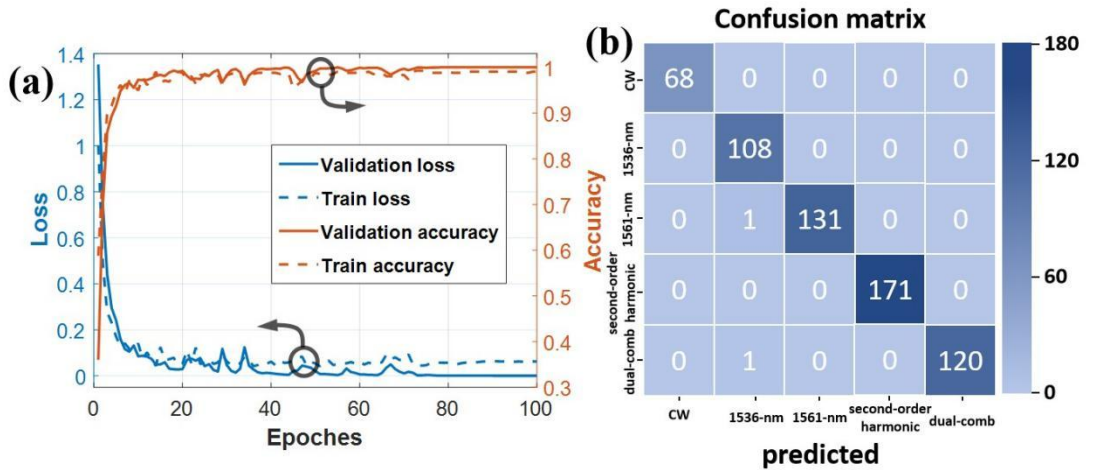


**Fig. S3.** (a) The curves of the loss and accuracy over epochs in the training process. (b) Confusion matrix for the CNN-Transformer hybrid model of 5 classification.

#### S4. The spectrum changes of 1536-nm and 1561-nm single-wavelength mode-locked states

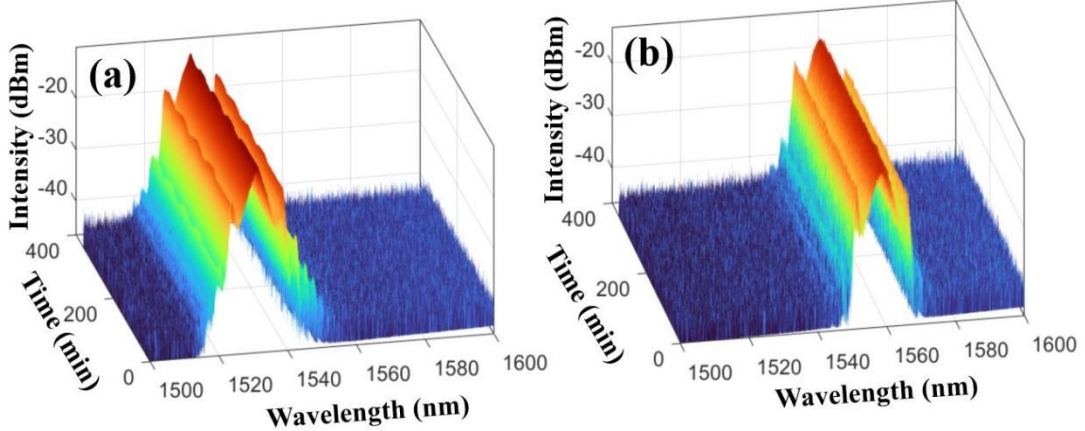


**Fig. S4.** The stability maintenance results of different mode-locked states including single-wavelength mode locking centered at (a) 1536 nm and (b) 1561 nm.

The stable single-wavelength mode-locked states are obtained by using the proposed developed evolutionary algorithm with the fitness function of single-wavelength mode locking. The CNN-Transformer network can be used to classify different single-wavelength mode-locked states such as 1536-nm mode locking and 1561-nm mode locking. The spectral changes of the proposed laser at the central wavelength of 1536 nm and 1561 nm are shown in Figure S4. They are easy to maintain for more than 6 hours of operation.